



Cite this: *Sustainable Food Technol.*, 2025, 3, 1986

Received 2nd July 2025  
Accepted 21st August 2025

DOI: 10.1039/d5fb00350d  
[rsc.li/susfoodtech](http://rsc.li/susfoodtech)

## Physical and functional properties of pulsed-ultraviolet treated starch based films with papaya leaf extract

T. Yin Feng,<sup>a</sup> M. I. Nur Hidayah,<sup>a</sup> F. Han Lyn  <sup>a</sup> and Z. A. Nur Hanani  <sup>a,b</sup>

This study developed corn starch (CS) films incorporating aqueous papaya leaf extract (PLE) and examined the effects of pulsed ultraviolet (PUV) treatment at 4, 12, and 15 J cm<sup>-2</sup> on their physical, mechanical, and antioxidant properties. PLE incorporation increased opacity, water contact angle, surface roughness, and antioxidant activity, but reduced solubility, water vapour permeability (WVP), and tensile strength. PUV treatment further decreased thickness, solubility, and WVP, while significantly ( $p < 0.05$ ) increasing tensile strength and reducing elongation at break, consistent with starch retrogradation and increased crystallinity. Colour, opacity, hydrophilicity, and antioxidant capacity, measured by total phenolic content (TPC) and DPPH scavenging, remained unaffected ( $p \geq 0.05$ ) by PUV. CS films containing PLE exhibited 90.45% higher TPC than pure CS films (control). Phenolic migration was greater in water than ethanol, reflecting the films' hydrophilic nature and faster release in aqueous environments. Overall, PUV treatment improved the mechanical durability of CS + PLE films without compromising antioxidant activity, supporting their potential as sustainable active packaging with tailored release for specific food systems.

### Sustainability spotlight

This study addresses the pressing issue of plastic pollution by developing a biodegradable corn starch-based film incorporating papaya leaf extract (PLE), an underutilized agricultural by-product. The use of pulsed ultraviolet (PUV) treatment enhances the film's tensile strength without compromising its antioxidant activities. By valorising agricultural waste and applying green processing technologies, this research contributes to the creation of a safe and sustainable food packaging solution. It supports a circular economy while reducing reliance on synthetic additives and petrochemical-based plastics. The work aligns with UN SDG 12 (Responsible Consumption and Production) and SDG 3 (Good Health and Well-being), advancing efforts to build sustainable food systems and reduce environmental impact.

## 1 Introduction

Bioactive compounds are naturally occurring phytochemicals that contribute to a plant's defence against diseases. Their concentration and composition vary among plant parts, including leaves, stems, bark, roots, wood, flowers, fruits, and seeds, and many have demonstrated antioxidant, antimicrobial, and other functional activities.<sup>1</sup> Extracts of such compounds from edible and medicinal plants have been used as food additives and are generally recognised as safe for human consumption.<sup>2</sup>

Papaya (*Carica papaya*), a member of the Caricaceae family, is among the most widely cultivated tropical fruit crops. In Malaysia, it ranks fourth in production volume after

watermelon, pineapple, and banana, with an output of 54 753 million metric tonnes in 2022.<sup>3</sup> The plant contains diverse phytochemicals, and most parts have recognised medicinal value. Papaya leaves are particularly rich in over 50 bioactive compounds, including glycosides, flavonoids, alkaloids, saponins, phenolics, amino acids, lipids, carbohydrates, enzymes, vitamins, and minerals, underpinning their broad therapeutic potential.<sup>4</sup> They exhibit stronger antioxidant and antibacterial activities than the seeds or fruit<sup>5</sup> and possess the highest total phenolic content (424.89 mg GAE/100 g dry mass), followed by unripe fruit, ripe fruit, and seeds.<sup>6</sup> Methanolic papaya leaf extracts contain phenolic acids (protocatechuic, *p*-coumaric, caffeoic, and chlorogenic acids) and flavonoids such as kaempferol, which contribute to antibacterial, antioxidant, anticancer, anti-inflammatory, and antifungal properties.<sup>5</sup> Traditionally, papaya leaves have been used in the treatment of malaria fever,<sup>7</sup> dengue fever,<sup>8</sup> and cancer.<sup>9</sup>

Increasing consumer demand for foods with high quality, safety, and nutritional value, and minimal synthetic additives,

<sup>a</sup>Department of Food Technology, Faculty of Food Science and Technology, Universiti Putra Malaysia, 43400 UPM Serdang, Selangor Darul Ehsan, Malaysia. E-mail: [hanani@upm.edu.my](mailto:hanani@upm.edu.my)

<sup>b</sup>Institute of Tropical Forestry and Forest Products, Universiti Putra Malaysia, 43400 UPM, Serdang, Selangor, Malaysia



has driven the development of active packaging. Unlike conventional packaging, which acts as a passive barrier, active packaging interacts with the food product to maintain quality, enhance safety, and extend shelf life. This can involve the controlled release of bioactive compounds, such as antioxidants or antimicrobial agents, derived from either synthetic or natural sources.<sup>10</sup> Plants are a valuable source of such compounds, including tannins, terpenoids, alkaloids, and flavonoids, many of which have demonstrated antimicrobial activity *in vitro*.<sup>11</sup>

Petrochemical-based plastics remain dominant in food packaging due to their low cost, light weight, inertness, and good barrier properties. However, they are non-biodegradable, and recent estimates indicate that more than 25.3 MMT of plastic waste enter the oceans annually, with 16.8 MMT sinking to the seabed or fragmenting into microplastics, 6.6 MMT floating as macroplastic debris, and 1.8 MMT accumulating on shorelines.<sup>12</sup> This has intensified interest in biodegradable polymers as sustainable alternatives.

Natural polymers such as polysaccharides, proteins, and lipids have been extensively studied for biodegradable active packaging.<sup>13</sup> Starch is particularly suitable due to its abundance, safety, biodegradability, and low environmental impact.<sup>14</sup> Corn starch (CS) exhibits excellent film-forming ability, primarily due to its high amylose content.<sup>15</sup> Incorporation of bioactive compounds into starch films can enhance their mechanical, barrier, antioxidant, antimicrobial, and pH-sensitive properties through interactions such as hydrogen bonding and electrostatic forces.

Ultraviolet (UV) irradiation is a non-thermal, low-cost, and environmentally friendly technology encompassing UV-A, UV-B, and UV-C wavelengths. Pulsed light technology delivers rapid, high-intensity bursts of broad-spectrum light, including a substantial UV-C component, generated by xenon flash lamps. Compared with continuous-wave UV systems, pulsed UV (PUV) offers shorter processing durations and eliminates the need for warm-up periods.<sup>16</sup> High doses of UV-C can improve protein-based films by promoting cross-linking between polymer chains *via* free radical formation, resulting in higher tensile strength, reduced solubility, and enhanced barrier properties.<sup>17</sup> UV irradiation has been applied to whey protein, soy protein, and gelatin films to achieve such improvements *via* covalent cross-linking and morphological modification.<sup>18,19</sup> However, most UV-modified packaging films have been based on protein systems or starch matrices without bioactive incorporation, and few studies have examined the effect of UV treatment on films containing plant-derived bioactives.

This study is novel in combining papaya leaf extract (PLE), a potent yet underutilised bioactive source, with PUV treatment in a CS film matrix. This approach differs from earlier work on plant-extract-based films or UV-modified starch systems by exploring the potential synergy between bioactive incorporation and irradiation to improve both functional (antioxidant) and structural (mechanical and barrier) properties. To the best of our knowledge, no previous study has investigated the combined effects of PLE incorporation and PUV treatment on starch-based films. Therefore, this work evaluates the physical, mechanical, barrier, and functional properties of PUV-treated

CS films containing PLE, with the aim of developing a biodegradable active packaging material with enhanced performance.

## 2 Method

### 2.1 Materials

Mature *C. papaya* leaves used were collected from the University Agriculture Park, Universiti Putra Malaysia. Corn starch and glycerol were purchased from Sigma-Aldrich (St. Louis, MO, USA). Folin Ciocalteu reagent was supplied by Merck and Co. (Darmstadt, Germany), while sodium carbonate and gallic acid were purchased from R&M Chemicals (Shah Alam, Malaysia). 2,2-Diphenyl-1-picrylhydrazyl (DPPH) was purchased from Tokyo Chemical Industry (Tokyo, Japan). Absolute ethanol (99.9% purity) was obtained from John Kollin Corporation (Midlothian, UK).

### 2.2 Preparation of papaya leaf extract (PLE)

The preparation of PLE was carried out according to Alonso *et al.*<sup>20</sup> with slight modifications. Fresh papaya leaves were washed with distilled water, air-dried at ambient temperature, and oven-dried at 50 °C for 2 d, until constant weight. The dried leaves were ground into powder and sieved to obtain a uniform particle size (<500 µm). The powder was extracted using a water to leaf ratio of 1:0.075 (v/w) and then heated to 70 °C for 20 min. The extract was filtered through a cheesecloth, followed by Whatman No. 1 filter paper (Maidstone, United Kingdom) under reduced pressure. The extract was then centrifuged at 3000×g for 10 min to remove fine colloidal particles, concentrated to 20°Brix under reduced pressure at 75 °C using a rotary evaporator (Eyela N-1001, Guangdong, China) and freeze-dried (Virtis Genesis 25, SP Industry Inc., Warminster, PA, USA). The resulting PLE powder was stored in an airtight amber bottle at 5 °C until use.

### 2.3 Preparation of film

CS film was prepared using the method by Zhang *et al.*<sup>21</sup> with slight modifications, as summarized in Fig. 1. CS (5.0 g) and glycerol (1.5 g) were dispersed in 93.5 mL of distilled water and stirred using a magnetic stirrer at 250 rpm for 40 min. The suspension was then heated to 96 °C to induce starch

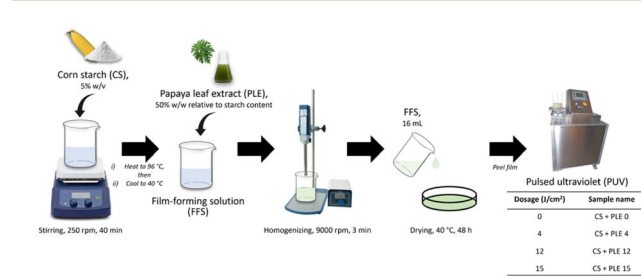


Fig. 1 Schematic diagram summarising the preparation of corn starch (CS)-based films with papaya leaf extracts (PLE) irradiated with different dosage (0, 4, 12, and 15 J cm<sup>-2</sup>) of pulse-ultraviolet (PUV) light.



gelatinisation, followed by cooling to 40 °C. PLE (2.5 g, 50% w/w relative to starch weight) was incorporated and homogenised at 9000 rpm for 3 min using a high-speed homogeniser (Heidolph Instruments GmbH & Co., Schwabach, Germany).

Aliquots of 16 mL of the film-forming solution were cast onto polystyrene Petri plates (14 × 14 cm) and dried at 40 °C for 48 h. Control films were prepared using the same procedure without PLE. Dried films were subjected to PUV treatment at fluences of 4, 12, and 15 J cm<sup>-2</sup> for 4 min using a pulsed ultraviolet system (XeMaticA-2L, SteriBeam, Gottmadingen, Germany). These dosages were selected based on preliminary screening, in which fluences above 15 J cm<sup>-2</sup> produced excessively brittle films unsuitable for packaging applications (data not shown). All films were conditioned in a dry cabinet (Che Scientific Co., Kwai Chung, Hong Kong) at 50 ± 5% relative humidity and 23 ± 2 °C for at least 48 h prior to characterisation.<sup>13</sup>

## 2.4 Physical properties of films

**2.4.1 Film thickness.** The thickness of the film was measured using a digital micrometre (Mitutoyo Absolute, Tester Sangyo Co. Ltd Japan). The film thickness was measured on ten randomly selected areas on the film and the mean thickness was calculated.

**2.4.2 Water solubility.** Water solubility of the films was determined according to the method of Maryam Adilah *et al.*<sup>13</sup> Film samples were cut into squares (2 × 2 cm) and dried in a hot-air oven (Memmert, Schwabach, Germany) at 100 ± 5 °C for 24 h to determine the initial dry mass ( $m_0$ ). The film samples were then immersed in 50 mL of distilled water and maintained at 23 ± 2 °C for 24 h. After immersion, the films were removed, blotted to remove excess surface water, and re-dried at 100 ± 5 °C for 24 h to determine the final dry mass ( $m_1$ ). Water solubility was calculated as:

$$\text{Water solubility (\%)} = \frac{m_0 - m_1}{m_0} \times 100$$

where  $m_0$  is the initial dry mass and  $m_1$  is the final dry mass after immersion.

**2.4.3 Water vapour permeability (WVP).** WVP of the film was determined according to the method of Maryam Adilah *et al.*<sup>13</sup> with slight modifications. Distilled water (6 mL) was placed into the crucible, and the film sample secured over the mouth of the crucible using vacuum seal grease applied around the rim to prevent leakage. The crucible was then placed in a desiccator maintained at 50 ± 5% relative humidity and 23 ± 2 °C. The weight of the crucible was recorded at 1 h intervals over a period of 9 h. WVP was calculated using the equation below:

$$\text{WVP (g m}^{-1} \text{ s}^{-1} \text{ Pa}^{-1}) = \frac{(W) \times (l)}{(A) \times (t) \times (\Delta P)}$$

where  $W$  is the weight loss of the crucible (g),  $l$  is the film thickness (m),  $A$  is the exposed film area (m<sup>2</sup>),  $t$  is time (s), and  $\Delta P$  is the partial water vapour pressure difference across the film (Pa).

**2.4.4 Mechanical properties.** Tensile strength (TS) and elongation at break (EAB) were determined according to the

ASTM D822-02 standard using an Instron 4302 Series IX testing machine (Instron Co., Canton, MA, USA).<sup>22</sup> Each strip was clamped between the machine grips with an initial gauge length of 30 mm and tested at a crosshead speed of 50 mm min<sup>-1</sup>, using a 5 kN load cell.

**2.4.5 Colour.** The colour of the films was determined using a MiniScan XE Plus Hunter colourimeter (Hunter Associates Laboratory. Inc. Reston, Virginia). The  $L$ ,  $a$  and  $b$  values were recorded, where  $L$  represent lightness (0 = black, 100 = perfect reflecting diffuser),  $a$  represents the red-green axis (positive = red, negative = green), and  $b$  represents the yellow-blue axis (positive = yellow, negative = blue). The colourimeter was calibrated before measurements using a standard white calibration tile.

**2.4.6 Opacity.** Film opacity was determined according to the method of Hamed *et al.*<sup>23</sup> with slight modifications. Films samples were cut into rectangular strips measuring 1 × 4 cm and placed inside a cuvette. The absorbance at 600 nm (Abs<sub>600</sub>) was measured using a Genesys 10 UV-vis spectrophotometer (Thermo Fisher Scientific, Madison, WI, USA). Film opacity was calculated using the following equation:

$$\text{Opacity (AU mm}^{-1}) = \frac{\text{Abs}_{600}}{x}$$

where  $x$  is the film thickness.

**2.4.7 Water contact angle (WCA).** The WCA was measured to determine the surface hydrophilicity of the films, following the method of Devi *et al.*<sup>24</sup> with slight modifications. One drop of 3 µL of ultrapure water was deposited on the film surface. The image of the droplet was measured using a digital microscope immediately.

**2.4.8 Atomic force microscopy (AFM).** Surface morphology of the film samples was analysed using Dimension Edge atomic force microscopy system with the ScanAsysts automatic image optimization technology (Bruker AXS GmbH, Karlsruhe, Germany). Scans were performed in tapping mode with a scan size of 10 µm and a scan rate of 6.00 µm s<sup>-1</sup>.

## 2.5 Antioxidant activity

**2.5.1 Total phenolic content (TPC).** The TPC of the films was determined following the method of Huda *et al.*<sup>25</sup> with slight modifications. Film samples (25 mg) were immersed in 3 mL of ethanol to obtain the extracts. An aliquot (0.5 mL) of the film extract was mixed with 2.5 mL of Folin-Ciocalteu reagent (10% v/v) and allowed to stand for 4 min at 23 ± 2 °C. Subsequently, 2 mL of sodium carbonate solution (7.5% w/v) was added, and the mixture was incubated for 2 h at 23 ± 2 °C. Absorbance was measured at 760 nm using a spectrophotometer. Gallic acid solutions (0–500 ppm) were used to construct the standard curve, and results were expressed as milligrams of gallic acid equivalent per gram film (mg GAE/g film).

**2.5.2 DPPH radical scavenging assay.** The DPPH radical scavenging activity of the films was determined according to the method of Huda *et al.*<sup>25</sup> Film samples (25 mg) were immersed in 3 mL of ethanol to obtain the extracts. An aliquot (3 mL) of the film extract was mixed with 1 mL of 0.1 mM ethanolic DPPH



solution, vortexed, and incubated in the dark at  $23 \pm 2$  °C for 30 min. The absorbance was then measured at 517 nm using a spectrophotometer. The DPPH radical scavenging activity was calculated using the following equation:

$$\text{DPPH radical scavenging activity (\%)} = \frac{(\text{Abs}_{\text{DPPH}} - \text{Abs}_{\text{extract}})}{\text{Abs}_{\text{DPPH}}}$$

## 2.6 Phenolic migration test

The migration of phenolic compounds from the films was evaluated according to the method of Piñeros-Hernandez<sup>26</sup> with slight modifications. Film sample ( $2 \times 2$  cm, 20 mg) were immersed in 5 mL of food simulant and shaken at 125 rpm at  $25 \pm 2$  °C for 7 d. Distilled water and 95% ethanol were selected as food simulants in accordance with the United States Food and Drug Administration (FDA) recommendations, representing aqueous and fatty food systems, respectively.<sup>27</sup> The concentration of phenolic compounds migrated into the simulants was determined using the TPC method described above.

## 2.7 Statistical analysis

All experiments were performed in triplicate ( $n = 3$ ), with results expressed as the mean  $\pm$  standard deviation. Statistical analysis was carried out using one-way ANOVA in Minitab (version 16.0), and significant differences between means ( $p < 0.05$ ) were identified using Tukey's post hoc test.

# 3 Results and discussion

## 3.1 Thickness

Film thickness directly influences key physical properties, including oxygen and water vapour transmission rates and mechanical strength, making accurate measurement essential.<sup>28</sup> As shown in Table 1, the control film was the thinnest ( $p < 0.05$ ) among all samples. This is consistent with previous studies which found that high amylose content facilitates the formation of compact structures, as the linear amylose chains interact readily to produce a dense polymer network.<sup>29,30</sup>

Incorporation of papaya leaf extract (PLE) significantly increased ( $p < 0.05$ ) the thickness of corn starch (CS) films. This increase can be attributed to structural disruption within the starch matrix, where PLE interferes with polymer–polymer

**Table 1** Thickness, and water solubility of corn starch (CS)-based films with papaya leaf extracts (PLE) irradiated with different dosage (0, 4, 12, and 15  $\text{J cm}^{-2}$ ) of pulse-ultraviolet (PUV) light<sup>a</sup>

Film	Thickness ( $\mu\text{m}$ )	Water solubility (%)
Control	$72.00 \pm 0.00^{\text{e}}$	$39.30 \pm 0.07^{\text{a}}$
CS + PLE 0	$110.00 \pm 0.00^{\text{a}}$	$35.38 \pm 0.18^{\text{b}}$
CS + PLE 4	$102.30 \pm 0.00^{\text{b}}$	$33.73 \pm 0.20^{\text{c}}$
CS + PLE 12	$90.00 \pm 0.00^{\text{c}}$	$28.62 \pm 0.16^{\text{d}}$
CS + PLE 15	$79.00 \pm 0.00^{\text{d}}$	$22.55 \pm 0.08^{\text{e}}$

<sup>a</sup> Means  $\pm$  standard deviation in the same column with different superscripts are significantly different.

interactions and introduces additional molecular structures that enlarge the matrix volume.<sup>31</sup> Similar effects have been observed in films containing plant-derived additives such as herbal powders, fruit peels, and medicinal plant extracts (e.g., *Aconitum heterophyllum*, *Artemisia annua*, and *Thymus serpyllum*), where solid particulates reinforce the matrix and increase thickness, whereas essential oils, being more miscible, generally do not cause significant changes.<sup>32,33</sup>

Conversely, PUV treatment significantly reduced film thickness ( $p < 0.05$ ), particularly at higher doses. The high amylose content and fine granule size of CS allow effective UV penetration,<sup>29</sup> which can promote starch retrogradation, leading to polymer chain realignment into crystalline domains. This rearrangement facilitates the expulsion and evaporation of water, plasticisers, and extract residues, producing a thinner and more compact film structure.<sup>34</sup>

## 3.2 Water solubility

Film solubility reflects its structural integrity and ability to resist interaction with water. A lower solubility usually indicates better water resistance. As shown in Table 1, the control CS film exhibited the highest solubility ( $p < 0.05$ ), which can be attributed to the intrinsic hydrophilicity of CS.<sup>34</sup> The presence of glycerol, a highly hydrophilic plasticiser containing three hydroxyl groups, further enhanced water affinity by forming hydrogen bonds with both starch chains and water molecules, thereby increasing solubility.<sup>35</sup> Incorporation of papaya leaf extract (PLE) significantly reduced solubility ( $p < 0.05$ ). This reduction is likely due to interactions between phenolic hydroxyl groups from the extract and hydroxyl groups of starch, which limit the availability of free hydroxyl sites for water binding.<sup>36</sup>

The resulting aggregation of intact granules and stronger intermolecular bonding further hindered water penetration. Similar reductions in solubility have been reported with starch films containing tea polyphenols<sup>36</sup> and lemon essential oil,<sup>32</sup> where phenolic or hydrophobic compounds interact with starch to reduce hydroxyl group availability. Such interactions, particularly with amylose, can promote the formation of semi-crystalline structures, hydrogen bonding networks, and inclusion complexes, thereby decreasing water uptake.<sup>37</sup>

PUV treatment also led to a dose-dependent decrease in solubility ( $p < 0.05$ ). High-amylose CS films exposed to higher PUV doses may undergo enhanced retrogradation, facilitating starch chain realignment, formation of dense crystalline regions, and water exclusion.<sup>38</sup> Retrograded high-amylose starch can achieve crystallinity levels of up to 40%, resulting in markedly lower solubility,<sup>34</sup> and in some cases forming resistant starch fractions that are virtually insoluble in water.<sup>39</sup>

## 3.3 Water vapour permeability (WVP)

WVP is a critical parameter in assessing the suitability of films for food packaging, as excessive moisture transfer can accelerate spoilage. As shown in Table 2, the control film exhibited the highest WVP ( $p < 0.05$ ), likely due to the abundance of free hydroxyl groups on its surface.<sup>40</sup> These hydroxyl groups readily



**Table 2** Water vapour permeability (WVP), water contact angle (WCA), tensile strength (TS), and elongation at break (EAB) of corn starch (CS)-based films with papaya leaf extracts (PLE) irradiated with different dosage (0, 4, 12, and 15 J cm<sup>-2</sup>) of pulse-ultraviolet (PUV) light<sup>a</sup>

Film	WVP ( $\times 10^{-8}$ g m <sup>-1</sup> s <sup>-1</sup> Pa <sup>-1</sup> )	WCA (°)	TS (MPa)	EAB (%)
Control	5.75 ± 0.09 <sup>a</sup>	43.44 ± 0.11 <sup>b</sup>	9.90 ± 1.00 <sup>a</sup>	67.42 ± 0.02 <sup>e</sup>
CS + PLE 0	3.89 ± 0.09 <sup>b</sup>	53.63 ± 0.08 <sup>a</sup>	3.90 ± 0.10 <sup>e</sup>	174.16 ± 0.01 <sup>a</sup>
CS + PLE 4	3.39 ± 0.06 <sup>c</sup>	53.19 ± 0.43 <sup>a</sup>	5.40 ± 0.40 <sup>d</sup>	149.15 ± 0.02 <sup>b</sup>
CS + PLE 12	2.83 ± 0.04 <sup>d</sup>	53.58 ± 0.53 <sup>a</sup>	6.90 ± 0.30 <sup>c</sup>	131.01 ± 0.00 <sup>c</sup>
CS + PLE 15	2.52 ± 0.07 <sup>e</sup>	53.77 ± 0.12 <sup>a</sup>	8.30 ± 0.40 <sup>b</sup>	123.47 ± 0.00 <sup>d</sup>

<sup>a</sup> Means ± standard deviation in the same column with different superscripts are significantly different ( $p < 0.05$ ).

form hydrogen bonds with water molecules, facilitating vapour transmission. Additionally, glycerol, while acting as a plasticiser, increases hydrophilicity and disrupts intra-molecular hydrogen bonding within the starch matrix, enlarging intermolecular spacing and creating a less dense network that favours moisture diffusion.<sup>41</sup>

Incorporation of PLE significantly reduced WVP ( $p < 0.05$ ), in agreement with the solubility results, where PLE incorporation also lowered water solubility. The phenolic hydroxyl groups in PLE form intermolecular hydrogen bonds with starch, increasing cross-linking density and reducing free volume in the polymer matrix.<sup>42</sup> This structural modification limits both water uptake, as reflected in lower solubility, and water vapour passage, leading to improved moisture barrier performance.<sup>43</sup> Nevertheless, further analyses such as FTIR might be performed to support this observation. Similar reductions in WVP have been reported with *Hibiscus sabdariffa* extract in potato starch films,<sup>44</sup> in which the WVP significantly decreased ( $p < 0.05$ ) from  $2.93$  to  $1.26 \times 10^{-10}$  g m<sup>-1</sup> s<sup>-1</sup> Pa<sup>-1</sup>. The incorporation of basil and green tea extracts have also been reported to lower the WVP of cassava starch films.<sup>45</sup>

PUV treatment further decreased WVP in a dose-dependent manner ( $p < 0.05$ ), also corroborating the solubility trend where higher irradiation dosages reduced water solubility. The likely mechanism is that PUV promotes starch retrogradation and crystallinity, producing a compact structure that resists both bulk water penetration and vapour diffusion.<sup>26</sup> Increased crystallinity has been linked to reduced permeability, as shown by Zhang and Rempel,<sup>46</sup> where increasing crystallinity from 6% to 9% lowered WVP from 1.2 to 0.9 g mm m<sup>-2</sup> h<sup>-1</sup> kPa<sup>-1</sup>. Similar effects have been observed in rice and corn starch films.<sup>47</sup>

### 3.4 Water contact angle (WCA)

The WCA assesses the surface hydrophilicity or hydrophobicity of films. Lower angles indicate greater wettability, with values below 65° typically denoting a hydrophilic surface while values above 90° are considered hydrophobic.<sup>36</sup> In this study, the initial WCA of all films was below 65° (Table 2), confirming their hydrophilic nature. The droplet size decreased rapidly after deposition, reflecting the films' capacity to absorb water. WCA can be influenced by surface roughness, sub-surface molecular interactions, hydrogen bond dynamics within the polymer matrix, and the material's surface energy.<sup>48</sup>

The control film had the lowest WCA (43.44°), indicating higher hydrophilicity than the PLE-incorporated film (53.63°). Native CS films are known for high water solubility and rapid water absorption,<sup>49</sup> consistent with the higher solubility and WVP observed. Incorporation of PLE significantly increased WCA ( $p < 0.05$ ), suggesting a reduction in surface wettability. This effect is likely due to phenolic compounds forming hydrogen bonds with starch chains, decreasing the availability of free hydroxyl groups for water interaction and slightly enhancing surface hydrophobicity.<sup>43,50</sup> Similar increases in WCA have been reported for cassava starch films with tea extract<sup>45</sup> and methylcellulose films with *Lippia alba* extract.<sup>50</sup>

PUV treatment did not significantly alter WCA across dosages ( $p \geq 0.05$ ), despite reducing solubility and WVP. This suggests that while PUV promotes retrogradation and crystalline structure formation within the bulk matrix, the molecular arrangement at the immediate surface, which determines WCA, remains largely unaffected.<sup>51</sup> According to Zisman,<sup>51</sup> surface wettability is dictated primarily by the chemical nature and packing of exposed surface molecules rather than the structure of underlying layers. Thus, PUV's impact on bulk hydrophilicity, which was evident in solubility and WVP results, did not translate into significant surface wettability changes.

### 3.5 Tensile strength and elongation at break

Tensile strength (TS) and elongation at break (EAB) are critical indicators of a film's ability to maintain integrity and withstand handling during food packaging applications. TS represents the maximum stress a film can endure before breaking, while EAB reflects its flexibility and capacity to deform under tensile load.<sup>40</sup>

The TS and EAB of the control CS films ranged from 3.90 to 9.90 MPa and 67.42 to 174.16%, respectively. These TS values are consistent with previous reports on plasticised CS films,<sup>52-54</sup> which range from 1 to 20 MPa depending on CS and glycerol concentrations. However, they remain lower than those of certain bioplastics such as polylactic acid (PLA), which typically exhibits TS values between 20 and 60 MPa,<sup>55-57</sup> but can be increased through reinforcement with fillers or co-polymers.

Control films achieved the highest TS but lowest EAB ( $p < 0.05$ ), consistent with the high amylose content of CS.<sup>58</sup> The linear structure of amylose enables strong intermolecular hydrogen bonding, creating a dense, ordered matrix with high tensile strength but limited chain mobility, thereby reducing



flexibility.<sup>47</sup> Glycerol, while acting as a plasticizer by spacing amylose chains and disrupting starch–starch interactions, still binds strongly to amylose, restricting excessive chain movement and maintaining strength.

Incorporation of PLE significantly reduced TS but increased EAB ( $p < 0.05$ ). This can be attributed to the partial replacement of strong starch–starch interactions with weaker starch–extract bonds,<sup>32</sup> and the creation of heterogeneous film domains with discontinuities,<sup>43</sup> which increases chain mobility. Phenolic compounds in PLE may act as secondary plasticizers,<sup>44,59</sup> similar to the reported effects of essential oils and plant extracts in other starch-based systems.<sup>43,59</sup> Hydrophilic polyphenols can also weaken hydrogen bonding within the starch matrix.<sup>32</sup>

PUV treatment of PLE-containing films increased TS and reduced EAB in a dose-dependent manner ( $p < 0.05$ ). This is consistent with PUV-induced starch retrogradation, which promotes crystalline region formation and densifies the polymer network.<sup>60</sup> Higher crystallinity improves mechanical strength but limits chain flexibility, thereby lowering EAB. Similar irradiation effects on polymer chain reorganisation have been reported in other biopolymer systems.<sup>61</sup>

Overall, the results suggest a trade-off between strength and flexibility, where PLE incorporation enhances elasticity but compromises strength, while PUV treatment restores strength at the expense of flexibility.

### 3.6 Colour

The visual appearance of packaging films influences consumer perception and acceptance of the packaged product. In this study, incorporation of PLE significantly decreased the  $L$  value compared to the control film ( $p < 0.05$ ), indicating a darker appearance (Table 3). This reduction in lightness is attributed to the intrinsic brownish hue of PLE, which contains naturally pigmented compounds. Similar darkening effects have been reported in corn starch films with microalgae<sup>30</sup> and fish gelatin films with tea extract.<sup>62</sup>

Films with PLE also showed significantly higher  $a$  and  $b$  values ( $p < 0.05$ ), indicating increased redness and yellowness. This shift is likely due to the presence of phenolic compounds, which impart brownish yellowish tones. Comparable colour changes were observed when mango peel extract, rich in  $\beta$ -carotene, was incorporated into gelatin films.<sup>60</sup>

PUV treatment at different dosages did not significantly affect  $L$ ,  $a$ , or  $b$  values compared to untreated PLE films ( $p \geq 0.05$ ).

0.05). While PUV promotes starch retrogradation and crystallinity, these structural changes do not appear to influence film colour. This agrees with Thakur *et al.*,<sup>47</sup> who found no significant colour differences in rice starch films with varying crystallinity levels.

### 3.7 Opacity

Light barrier properties are important for food packaging as they protect products from visible and UV light, both of which can accelerate oxidation and quality degradation. As shown in Table 3, PLE incorporation significantly increased film opacity ( $p < 0.05$ ). This can be attributed to light scattering from extract particles, as well as the presence of naturally coloured compounds such as phenolic compounds.<sup>60</sup> Similar increases in opacity have been reported in cassava films containing pumpkin residue extract and oregano essential oil,<sup>63</sup> and in fish gelatin films with tea extract.<sup>62</sup> Grape pomace extract, rich in phenolics, has likewise been shown to increase the opacity of tapioca starch films.<sup>64</sup>

In addition, PLE incorporation increased film thickness (Table 1), which further reduced transparency, consistent with reports by Adilah *et al.*<sup>60</sup> in gelatin films incorporated with mango kernel extract. While PUV treatment probably induced starch retrogradation and increased crystallinity, no significant changes in opacity were observed across dosages ( $p \geq 0.05$ ). This agrees with Thakur *et al.*,<sup>47</sup> who found no direct relationship between starch film crystallinity and opacity. Overall, increasing film opacity through PLE addition may provide functional benefits for light-sensitive foods by reducing exposure to UV and visible light, which can delay oxidative spoilage.<sup>60</sup>

### 3.8 Atomic force microscopy (AFM)

AFM images (Fig. 2) reveal the surface topography of the films. Pure CS film (control) showed the lowest value in roughness suggested that the film exhibited a smooth and homogenous surface. This is consistent with the ability of amylose-rich corn starch to form a compact, dense, and ordered polymer matrix.<sup>59</sup> Similar results have been reported for pure alginate films.<sup>30</sup>

Incorporation of PLE increased surface roughness from 3.00 to 14.60 nm (Table 4), likely due to the deposition of extract particles on the film surface and disruption of the polymer network.<sup>65</sup> Comparable effects have been observed with blueberry extract in corn starch films<sup>48</sup> and lycopene in cassava

**Table 3**  $L$ ,  $a$ ,  $b$ , and opacity values of corn starch (CS)-based films with papaya leaf extracts (PLE) irradiated with different dosage (0, 4, 12, and 15  $\text{J cm}^{-2}$ ) of pulse-ultraviolet (PUV) light<sup>a</sup>

Film	$L$	$a$	$b$	Opacity ( $\text{AU mm}^{-1}$ )
Control	$82.63 \pm 0.03^{\text{a}}$	$1.64 \pm 0.04^{\text{b}}$	$-3.04 \pm 0.02^{\text{b}}$	$0.33 \pm 0.01^{\text{b}}$
CS + PLE 0	$74.46 \pm 0.02^{\text{b}}$	$4.13 \pm 0.02^{\text{a}}$	$23.41 \pm 0.02^{\text{a}}$	$0.40 \pm 0.00^{\text{a}}$
CS + PLE 4	$74.46 \pm 0.04^{\text{b}}$	$4.13 \pm 0.01^{\text{a}}$	$23.41 \pm 0.01^{\text{a}}$	$0.41 \pm 0.00^{\text{a}}$
CS + PLE 12	$74.51 \pm 0.01^{\text{b}}$	$4.14 \pm 0.01^{\text{a}}$	$23.43 \pm 0.02^{\text{a}}$	$0.41 \pm 0.00^{\text{a}}$
CS + PLE 15	$74.44 \pm 0.02^{\text{b}}$	$4.15 \pm 0.01^{\text{a}}$	$23.40 \pm 0.01^{\text{a}}$	$0.41 \pm 0.00^{\text{a}}$

<sup>a</sup> Means  $\pm$  standard deviation in the same column with different superscripts are significantly different ( $p < 0.05$ ).



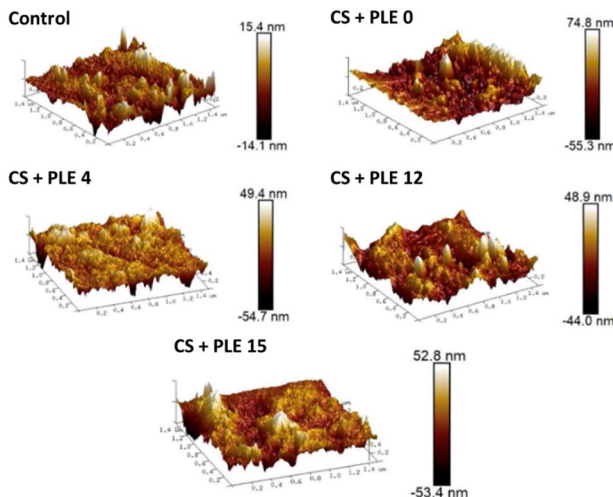


Fig. 2 Atomic force microscopy analysis corn starch (CS)-based films with papaya leaf extracts (PLE) irradiated with different dosage ( $0, 4, 12$ , and  $15 \text{ J cm}^{-2}$ ) of pulse-ultraviolet (PUV) light.

Table 4 Average surface roughness of corn starch (CS)-based films with papaya leaf extracts (PLE) irradiated with different dosage ( $0, 4, 12$ , and  $15 \text{ J cm}^{-2}$ ) of pulse-ultraviolet (PUV) light

Film	Average surface roughness (nm)
Control	3.00
CS + PLE 0	14.60
CS + PLE 4	7.10
CS + PLE 12	7.09
CS + PLE 15	7.11

starch films,<sup>65</sup> both of which produced coarse, discontinuous surfaces. Nunes *et al.*<sup>50</sup> also reported surface imperfections in methylcellulose films after *L. alba* extract addition.

The increased roughness of PLE films may have contributed to the higher water contact angles, as surface corrugations can increase apparent hydrophobicity.<sup>66</sup> PUV treatment, however, reduced roughness for about 51% compared to untreated PLE (CS + PLE 0). This is likely due to retrogradation-driven water and extract evaporation, followed by collapse of pore structures into a more compact, ordered surface.<sup>46,67</sup> Increasing PUV dosage did not produce further significant changes ( $p \geq 0.05$ ), suggesting that surface smoothing occurs primarily in the early stages of treatment.

### 3.9 Antioxidant activity

TPC and DPPH assay were performed to assess the antioxidant properties of the films. TPC quantifies phenolic compounds while the DPPH assay evaluates the radical scavenging capacity of antioxidants toward free radicals.

As shown in Fig. 3, incorporation of PLE significantly increased ( $p < 0.05$ ) the TPC of corn starch films by 90.45% compared to the control, consistent with previous findings that papaya leaf extract contains high phenolic levels.<sup>68</sup> Water-

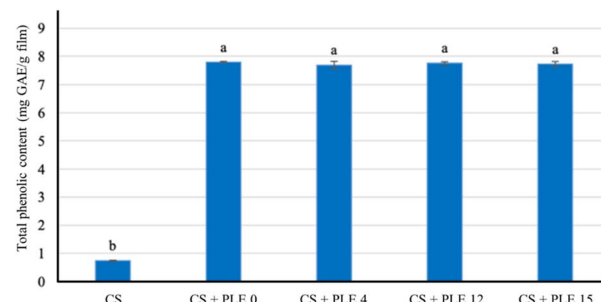


Fig. 3 Total phenolic content of corn starch (CS)-based films with papaya leaf extracts (PLE) irradiated with different dosage ( $0, 4, 12$ , and  $15 \text{ J cm}^{-2}$ ) of pulse-ultraviolet (PUV) light.

extracted PLE in particular has been reported to yield higher polyphenol concentrations and stronger scavenging activity than organic solvent extracts. Similar trends have been observed in films incorporating other plant-derived antioxidants, such as green tea, durian leaf, red grape seed, coconut water, and *Ziziphora clinopodioides* essential oil, all of which impart antioxidant and antimicrobial properties to active packaging.<sup>30,69,70</sup>

DPPH results (Fig. 4) showed that PLE-containing films exhibited markedly higher radical scavenging activity than the control ( $p < 0.05$ ). The polyphenols in PLE are capable of donating electrons to neutralise reactive free radicals, producing the stable diphenylpicrylhydrazine (yellow) product.<sup>68</sup> The DPPH radical scavenging activities demonstrated a similar trend with the TPC, which aligns with earlier studies reporting a positive correlation between phenolic content and antioxidant activity.<sup>71</sup>

PUV treatment, regardless of dosage, did not significantly alter TPC or DPPH activity ( $p \geq 0.05$ ), suggesting that phenolic compounds remained stable under treatment. This stability may be attributed to flavonoids such as kaempferol and quercetin in papaya leaf, which can potentially absorb UV and mitigate photodegradation.<sup>72</sup> Therefore, incorporating PLE into biodegradable films not only enhances antioxidant activity but may also protect sensitive food products, particularly those high in lipids, by preventing autoxidation and inhibiting lipoxygenase activity.<sup>73</sup>

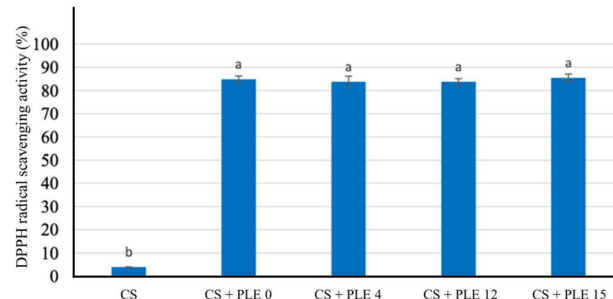


Fig. 4 DPPH radical scavenging activity of corn starch (CS)-based films with papaya leaf extracts (PLE) irradiated with different dosage ( $0, 4, 12$ , and  $15 \text{ J cm}^{-2}$ ) of pulse-ultraviolet (PUV) light.

### 3.10 Phenolic migration test

Active compounds in functional packaging can migrate to the food surface or through the headspace. Release from a polymeric matrix typically follows three stages: (i) absorption of the food simulant, causing polymer swelling; (ii) relaxation of the polymer network, increasing permeability; and (iii) diffusion of active compounds into the surrounding medium.<sup>74</sup> The rate and extent of migration depend on the compatibility between the active compound, the polymer, and the food simulant, as well as the polymer's solubility and swelling behaviour.

As shown in Fig. 5, phenolic migration from CS + PLE films was higher in distilled water than in 95% ethanol. This trend aligns with the films' hydrophilic nature and higher solubility in aqueous media. In water, the film rapidly absorbs moisture, leading to swelling, weakening of the polymer network, and enhanced release of phenolic compounds.<sup>13</sup> Prolonged immersion (7 days) in water resulted in extensive structural disruption, with many samples completely dissolving, consistent with previous observations in hydrophilic films containing soy protein isolate, fish gelatin, ethylene-vinyl alcohol copolymer, and starch-chitosan incorporated with antioxidants.<sup>13,75,76</sup>

In contrast, migration into ethanol was much lower, and the films remained structurally intact. This is attributed to the relatively lower swelling of starch in ethanol, which limits simulant penetration into the film matrix.<sup>26</sup>

The distinct release profiles have application-specific implications. Rapid phenolic migration in aqueous environments may be advantageous for high-moisture foods, enabling immediate antioxidant and antimicrobial action to delay oxidative and microbial spoilage. Conversely, the slower release in fatty simulants suggests potential for sustained antioxidant activity in lipid-rich foods, extending protection during storage. Such selective release behaviour allows CS + PLE films to be tailored for targeted food preservation strategies.

## 4 Conclusion

This study showed that incorporating PLE into CS films significantly increased ( $p < 0.05$ ) film thickness, opacity, and antioxidant activity, while reducing solubility, water vapour permeability (WVP), and tensile strength. PUV treatment

further modified these properties. Increasing PUV dosage led to reduced thickness, solubility, WVP, and surface roughness, while significantly increasing ( $p < 0.05$ ) tensile strength and reducing elongation at break, consistent with starch retrogradation and increased crystallinity. Notably, PUV treatment did not significantly affect colour parameters ( $L$ ,  $a$ ,  $b$ ), opacity, surface hydrophobicity, or antioxidant activity. The stable TPC and DPPH scavenging activity after PUV exposure indicate that PLE's bioactive compounds are UV-tolerant, likely due to the protective role of flavonoids. Migration testing revealed higher phenolic release in aqueous simulants than in ethanol, correlating with the films' hydrophilic nature and higher solubility in water. This selective migration suggests potential applications tailored to food moisture content, offering rapid phenolics release for high-moisture foods and slower, sustained release for lipid-rich products.

However, further work is required to address key limitations. The mechanical durability of the films under real handling and storage conditions, their performance with actual food products, and the long-term stability of phenolic compounds during storage remain to be evaluated. Industrial adoption of PUV treatment may also be constrained by equipment cost, processing throughput, and uniformity of UV exposure. In addition, while migration testing was performed using FDA-recommended food simulants, comprehensive regulatory compliance testing such as EU 10/2011, will be essential before commercial application. Overall, PUV treatment offers a promising strategy to enhance the mechanical performance of CS-based active films without diminishing their antioxidant functionality, paving the way for their use in sustainable, functional food packaging.

## Author contributions

Yin Feng, T.: writing- original draft, data curation, formal analysis, investigation, and project administration. Nur Hidayah, M. I.: data curation and writing – original draft. Han Lyn, F.: writing, reviewing and editing, and data curation. Nur Hanani, Z. A.: conceptualization, data curation, writing – reviewing, validation, supervision, resource provision, project administration, and funding acquisition.

## Conflicts of interest

There are no conflicts to declare.

## Data availability

All data are contained within the article.

## Acknowledgements

The authors would like to thank the University Agricultural Park for providing the papaya leaves and Universiti Putra Malaysia (UPM) for the facilities provided.

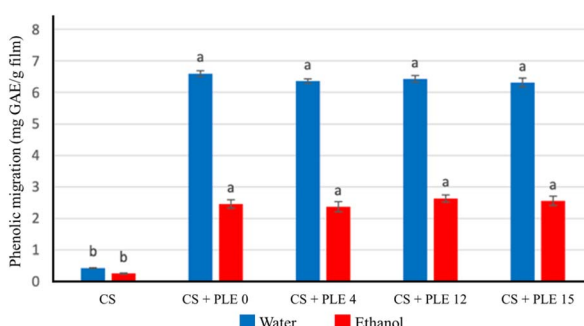


Fig. 5 Phenolic migration of corn starch (CS)-based films with papaya leaf extracts (PLE) irradiated with different dosage (0, 4, 12, and 15  $\text{J cm}^{-2}$ ) of pulse-ultraviolet (PUV) light in water and 95% ethanol.



## References

1 J. Lohidas, S. Manjusha, G. Glory and G. Jothi, *Plant Arch.*, 2015, **15**, 1179–1186.

2 M. B. Soquette, L. de M. Terra and C. P. Bastos, *CyTA - J. Food*, 2018, **16**, 400–412.

3 Ministry of Agriculture and Food Security, *Malaysia Agrofood in Figures 2022*, Putrajaya, Malaysia, 2023.

4 A. Sharma, R. Sharma, M. Sharma, M. Kumar, M. D. Barbhai, J. M. Lorenzo, S. Sharma, M. K. Samota, M. Atanassova, G. Caruso, Mo. Naushad, Radha, D. Chandran, P. Prakash, M. Hasan, N. Rais, A. Dey, D. K. Mahato, S. Dhumal, S. Singh, M. Senapathy, S. Rajalingam, M. Visvanathan, L. A. K. Saleena and M. Mekhemar, *Oxid. Med. Cell. Longevity*, 2022, **2022**, 1–20.

5 S. Arumugam, G. Pugazhenthi and S. selvaraj, *Mater. Today: Proc.*, 2023, DOI: [10.1016/j.matpr.2023.02.256](https://doi.org/10.1016/j.matpr.2023.02.256).

6 A. Maisarah, R. Asmah and O. Fauziah, *J. Tissue Sci. Eng.*, 2023, DOI: [10.1016/j.matpr.2023.02.256](https://doi.org/10.1016/j.matpr.2023.02.256).

7 A. Afzan, N. R. Abdullah, S. Z. Halim, B. A. Rashid, R. H. R. Semail, N. Abdullah, I. Jantan, H. Muhammad and Z. Ismail, *Molecules*, 2012, **17**, 4326–4342.

8 N. Ahmad, H. Fazal, M. Ayaz, B. H. Abbasi, I. Mohammad and L. Fazal, *Asian Pac. J. Trop. Biomed.*, 2011, **1**, 330–333.

9 N. Otsuki, N. H. Dang, E. Kumagai, A. Kondo, S. Iwata and C. Morimoto, *J. Ethnopharmacol.*, 2010, **127**, 760–767.

10 S. Seyyedi-Mansour, M. Carpene, P. Barciela, A. Perez-Vazquez, E. Assadpour, M. A. Prieto and S. M. Jafari, *Adv. Colloid Interface Sci.*, 2025, **340**, 103457.

11 E. Dagne, B. Dobo and Z. Bedewi, *Pharmacogn. J.*, 2021, **13**, 1727–1733.

12 N. Isobe, S. Ishii and H. Nomaki, *Curr. Opin. Chem. Eng.*, 2025, **47**, 101089.

13 Z. A. Maryam Adilah, B. Jamilah and Z. A. Nur Hanani, *Food Hydrocolloids*, 2018, **74**, 207–218.

14 N. Yang, H. Sha, W. Bi, S. Li, S. Wu and D. Su, *Food Packag. Shelf Life*, 2025, **47**, 101427.

15 Y. Yu, J. Xu, J. Xu, Y. Li, X. Zhang and W. Zhang, *Int. J. Biol. Macromol.*, 2025, **303**, 140734.

16 V. M. Gómez-López, T. Koutchma and K. Linden, in *Novel Thermal and Non-Thermal Technologies for Fluid Foods*, Elsevier, 2012, pp. 185–223.

17 M. Uyarcan and S. C. Güngör, *Int. J. Biol. Macromol.*, 2024, **282**, 137085.

18 T. Akter, M. Shakil and T. Mahawanich, *Future Foods*, 2025, **11**, 100663.

19 V. P. Romani, P. C. Martins, M. da Rocha, M. C. S. Bulhosa, F. Kessler and V. G. Martins, *Antioxidants*, 2024, **13**, 517.

20 N. C. Alonso, G. R. Sala, A. B. Sanahuja and A. V. García, *Ind. Crops Prod.*, 2025, **224**, 120395.

21 Y. Zhang, Z. Li, J. Zeng, H. Gao and J. Qi, *Food Hydrocolloids*, 2025, **164**, 111195.

22 ASTM, *D 882-02: Standard Test Method for Tensile Properties of Thin Plastic Sheeting*, ASTM International, Philadelphia, PA, 2002.

23 Y. S. Hamed, K. R. Hassan, H. M. Ahsan, M. Hussain, Abdullah, J. Wang, X. G. Zou, T. Bu, A. M. Rayan and K. Yang, *Food Chem.*, 2024, **457**, 140059.

24 N. Devi, G. Shayoraj, S. A. Shivani, S. K. Dubey, S. Sharma and S. Kumar, *Carbohydr. Res.*, 2025, **550**, 109404.

25 K. U. Huda, A. Ahmad, Z. Mushtaq, M. A. Raza, A. Moreno, F. Saeed and M. Afzaal, *Int. J. Biol. Macromol.*, 2025, **306**, 141558.

26 D. Piñeros-Hernandez, C. Medina-Jaramillo, A. López-Córdoba and S. Goyanes, *Food Hydrocolloids*, 2017, **63**, 488–495.

27 Guidance for Industry: Preparation of Premarket Submissions for Food Contact Substances (Chemistry Recommendations) | FDA, <https://www.fda.gov/regulatory-information/search-fda-guidance-documents/guidance-industry-preparation-premarket-submissions-food-contact-substances-chemistry>, (accessed 30 June 2025).

28 P. Kumar, R. Tanwar, V. Gupta, A. Upadhyay, A. Kumar and K. K. Gaikwad, *Int. J. Biol. Macromol.*, 2021, **187**, 223–231.

29 L. Zhang, L. Zhong, P. Wang, L. Zhan, Y. Yangzong, T. He, Y. Liu, D. Mao, X. Ye, Z. Cui, Y. Huang and Z. Li, *Foods*, 2023, **12**, 3157.

30 M. J. Fabra, M. Martínez-Sanz, L. G. Gómez-Mascaraque, R. Gavara and A. López-Rubio, *Carbohydr. Polym.*, 2018, **186**, 184–191.

31 P. Tongnuanchan, S. Benjakul and T. Prodpran, *Int. Aquat. Res.*, 2014, **6**, 1–12.

32 X. Song, G. Zuo and F. Chen, *Int. J. Biol. Macromol.*, 2018, **107**, 1302–1309.

33 A. Ali, A. Basit, A. Hussain, S. Sammi, A. Wali, G. Goksen, A. Muhammad, F. Faiz, M. Trif, A. Rusu and M. F. Manzoor, *Front. Nutr.*, 2023, **9**, 1066337.

34 A. Soler, G. Velazquez, R. Velazquez-Castillo, E. Morales-Sánchez, P. Osorio-Díaz and G. Méndez-Montealvo, *Carbohydr. Res.*, 2020, **497**, 108137.

35 E. E. Sirbu, A. Dinita, M. Tănase, A. I. Portocă, A. Bondarev, C. E. Enascuta and C. Calin, *Processes*, 2024, **12**, 2021.

36 M. Feng, L. Yu, P. Zhu, X. Zhou, H. Liu, Y. Yang, J. Zhou, C. Gao, X. Bao and P. Chen, *Carbohydr. Polym.*, 2018, **196**, 162–167.

37 J. Pan, C. Li, J. Liu, Z. Jiao, Q. Zhang, Z. Lv, W. Yang, D. Chen and H. Liu, *Foods*, 2024, **13**, 3896.

38 C. Zhiguang, Z. Rui, Y. Qi and Z. Haixia, *Int. J. Food Sci. Technol.*, 2023, **58**, 4519–4528.

39 Q. Chang, B. Zheng, Y. Zhang and H. Zeng, *Int. J. Biol. Macromol.*, 2021, **186**, 163–173.

40 T. Frangopoulos, A. Marinopoulou, A. Goulas, E. Likotrafiti, J. Rhoades, D. Petridis, E. Kannidou, A. Stamelos, M. Theodoridou, A. Arampatzidou, A. Tosounidou, L. Tsekmes, K. Tsichlakis, G. Gkikas, E. Tourasanidis and V. Karageorgiou, *Foods*, 2023, **12**, 2812.

41 E. Basiak, A. Lenart and F. Debeaufort, *Polymers*, 2018, **10**, 412.

42 N. Suderman, M. I. N. Isa and N. M. Sarbon, *Food Biosci.*, 2018, **24**, 111–119.

43 L. Li, H. Chen, M. Wang, X. Lv, Y. Zhao and L. Xia, *Carbohydr. Polym.*, 2018, **194**, 395–400.



44 A. M. Cruz-Gálvez, J. Castro-Rosas, M. L. Rodríguez-Marín, A. Cadena-Ramírez, A. Tellez-Jurado, X. Tovar-Jiménez, E. A. Chavez-Urbiola, A. Abreu-Corona and C. A. Gómez-Aldapa, *LWT*, 2018, **93**, 300–305.

45 C. Medina-Jaramillo, O. Ochoa-Yepes, C. Bernal and L. Famá, *Carbohydr. Polym.*, 2017, **176**, 187–194.

46 Y. Zhang and J. H. Han, *J. Food Sci.*, 2010, **75**, N8–N16.

47 R. Thakur, P. Pristijono, J. B. Golding, C. E. Stathopoulos, C. Scarlett, M. Bowyer, S. P. Singh and Q. V. Vuong, *Starch - Staerke*, 2018, **70**, 1700099.

48 T. J. Gutiérrez and V. A. Alvarez, *Food Hydrocolloids*, 2018, **77**, 407–420.

49 H. R. Arifin, M. Djali, B. Nurhadi, S. A. Hasim, A. Hilmi and A. V. Puspitasari, *Int. J. Food Prop.*, 2022, **25**, 509–521.

50 M. R. Nunes, M. de Souza Maguerroski Castilho, A. P. de Lima Veeck, C. G. da Rosa, C. M. Noronha, M. V. O. B. Maciel and P. M. Barreto, *Carbohydr. Polym.*, 2018, **192**, 37–43.

51 W. A. Zisman, *Adv. Chem.*, 1964, **23**, 1–51.

52 W. Abotbina, S. M. Sapuan, M. T. H. Sultan, M. F. M. Alkbir and R. A. Ilyas, *Polymers*, 2021, **13**, 3487.

53 A. Safitri, P. S. D. Sinaga, H. Nasution, H. Harahap, Z. Masyithah, Iriany and R. Hasibuan, *IOP Conf. Ser. Earth Environ. Sci.*, 2022, **1115**, 012076.

54 N. N. Nasir and S. A. Othman, *J. Phys. Sci.*, 2021, **32**, 89–101.

55 G. Gao, F. Xu, J. Xu and Z. Liu, *Materials*, 2022, **15**(19), 7039.

56 F. Han Lyn, M. R. Ismail-Fitry, M. A. Noranizan, T. B. Tan and Z. A. Nur Hanani, *Int. J. Biol. Macromol.*, 2024, **266**, 131340.

57 A. Moldovan, S. Cuc, D. Prodan, M. Rusu, D. Popa, A. C. Taut, I. Petean, D. Bomboş, R. Doukeh and O. Nemes, *Polymers*, 2023, **15**, 2855.

58 C. L. Luchese, J. C. Spada and I. C. Tessaro, *Ind. Crops Prod.*, 2017, **109**, 619–626.

59 A. Nouri, M. Tavakkoli Yaraki, M. Ghorbanpour and S. Wang, *Int. J. Biol. Macromol.*, 2018, **115**, 227–235.

60 A. N. Adilah, B. Jamilah, M. A. Noranizan and Z. A. N. Hanani, *Food Packag. Shelf Life*, 2018, **16**, 1–7.

61 A. Ashfaq, J. C. An, P. Ulański and M. Al-Sheikhly, *Pharmaceutics*, 2021, **13**, 1765.

62 K. Nilsawan, S. Benjakul and T. Prodpran, *Food Hydrocolloids*, 2018, **80**, 212–221.

63 K. dos Santos Caetano, N. Almeida Lopes, T. M. Haas Costa, A. Brandelli, E. Rodrigues, S. Hickmann Flôres and F. Cladera-Olivera, *Food Packag. Shelf Life*, 2018, **16**, 138–147.

64 Y. Xu, N. Rehmani, L. Alsubaie, C. Kim, E. Sismour and A. Scales, *Food Packag. Shelf Life*, 2018, **16**, 86–91.

65 R. Q. Assis, S. M. Lopes, T. M. H. Costa, S. H. Flôres and A. de O. Rios, *Ind. Crops Prod.*, 2017, **109**, 818–827.

66 K. Y. Law, *Acc. Mater. Res.*, 2022, **3**, 1–7.

67 F. M. Pelissari, M. M. Andrade-Mahecha, P. J. do A. Sobral and F. C. Menegalli, *J. Colloid Interface Sci.*, 2017, **505**, 154–167.

68 Q. V. Vuong, S. Hirun, P. D. Roach, M. C. Bowyer, P. A. Phillips and C. J. Scarlett, *J. Herb. Med.*, 2013, **3**, 104–111.

69 W. Y. Joanne Kam, H. Mirhosseini, F. Abas, N. Hussain, S. Hedayatnia and H. L. Florence Chong, *Food Control*, 2018, **90**, 66–72.

70 P. Rodsamran and R. Sothornvit, *Food Hydrocolloids*, 2018, **79**, 243–252.

71 Y. Shahbazi, *Int. J. Biol. Macromol.*, 2017, **99**, 746–753.

72 E. B. M. Younis, A. G. M. N. Hasaneen and H. M. M. Abdel-Aziz, *Plant Signaling Behav.*, 2010, **5**, 1197.

73 A. J. McEvily, R. Iyengar and A. T. Gross, *American Chemical Society*, ed. C.-T. Ho, C. Y. Lee and M.-T. Huang, Washington, USA, 1992, pp. 318–325.

74 R. Cerruti da Costa, A. Paula Ineichen, C. da Silva Teixeira, I. Casagrande Bellettini and L. Nardini Carli, *Polímeros*, 2022, **32**(3), e2022028.

75 M. Calatayud, C. López-De-Dicastillo, G. López-Carballo, D. Vélez, P. Hernández Muñoz and R. Gavara, *Food Chem.*, 2013, **139**, 51–58.

76 E. Talón, K. T. Trifkovic, M. Vargas, A. Chiralt and C. González-Martínez, *Carbohydr. Polym.*, 2017, **175**, 122–130.

